Numerical computation of the cut locus via a variational approximation of the distance function

François Générau, Edouard Oudet, Bozhidar Velichkov

ESAIM: M2AN 56 (2022) 105–120
https://doi.org/10.1051/m2an/2021088

ESAIM: Mathematical Modelling and Numerical Analysis
www.esaim-m2an.org

NUMERICAL COMPUTATION OF THE CUT LOCUS *VIA* A VARIATIONAL APPROXIMATION OF THE DISTANCE FUNCTION

François Générau[1], Edouard Oudet[2,*] and Bozhidar Velichkov[3]

Abstract. We propose a new method for the numerical computation of the cut locus of a compact submanifold of $\mathbb{R}^3$ without boundary. This method is based on a convex variational problem with conic constraints, with proven convergence. We illustrate the versatility of our approach by the approximation of Voronoi cells on embedded surfaces of $\mathbb{R}^3$.

Mathematics Subject Classification. 49J45, 35R35, 49M05, 35J25.

Received June 16, 2020. Accepted December 20, 2021.

1. Introduction

Let S be a compact real analytic surface without boundary embedded in $\mathbb{R}^3$, and let $b \in S$ be any point of S (that can be thought of as a base point).

Definition 1.1. The *cut locus* of b in S can be defined as the closure of the set of points $p \in S$ such that there exist at least two minimizing geodesics of S between p and b. We will denote it by $\mathrm{Cut}_b(S)$. Equivalently, it is also the set of points of $S \setminus \{b\}$ around which the distance function to the point b – denoted by d_b – is not smooth.

The cut locus is a fundamental object in Riemannian geometry, and it is a natural problem to try and find ways to compute it numerically. In this paper, we propose a numerical approximation of $\mathrm{Cut}_b(S)$, based on a convex variational problem on S, with proven convergence. It is not trivial to compute $\mathrm{Cut}_b(S)$ because it is not stable with respect to C^1-small variations of S. See for instance Example 2 of [1]. In particular, one can't approximate the cut locus of S with the cut locus of a piecewise linear approximation of S.

Related works. Let us review the techniques used in the past by different authors to approximate the cut locus. We may divide them into two categories.

Geodesic approximation on parametrized surfaces. This approach was used in [14, 18]. In [18], on genus 1 parametrized surfaces, the authors computed a degree 4 polynomial approximation of the exponential map

Keywords and phrases. Calculus of variation, cut locus, relaxation, manifold.

[1] Laboratoire Jean Kuntzmann (LJK), Université Joseph Fourier, Bâtiment IMAG, 700 Avenue Centrale, 38041 Grenoble Cedex 9, France.

[2] Laboratoire Jean Kuntzmann (LJK), Université Grenoble Alpes, Bâtiment IMAG, 700 Avenue Centrale, 38041 Grenoble Cedex 9, France.

[3] Dipartimento di Matematica, Università di Pisa, Largo Bruno Pontecorvo, 5, 56127 Pisa, Italy.

*Corresponding author: edouard.oudet@univ-grenoble-alpes.fr

using the geodesic equation and deduced an approximation of the cut locus from there. In [14], the authors used the deformable simplicial complexes (DSC) method and finite differences techniques for geodesic computations to compute geodesic circles of increasing radius and their self-intersections, *i.e.* the cut locus. They applied the method to genus 1 surfaces. These papers contain no proof of convergence of the computed cut locus.

Exact geodesic computation on discretized surfaces. This approach was used in [9, 13]. In [13], the authors computed the geodesics on a convex triangulated surface. They deduced an approximation of the cut locus of the triangulated surface and filtered it according to the angle formed by the geodesics meeting at a point of the approximated cut locus, to make their approximation stable. They applied the method to ellipsoids. There is no proof of convergence. In [9], the authors computed shortest curves on a graph obtained from a sufficiently dense sample of points of the surface. From there they deduced an approximation of the cut locus and filtered it according to the maximal distance (called *spread*) between the geodesics meeting at a point of the approximated cut locus. They proved that the set they compute converges to the cut locus (see [9], Thm. 4.1).

We may also mention [4], where the authors used some more geometric tools to compute (numerically) the cut locus of an ellipsoid or a sphere with some particular metric with singularities.

Our method. A natural approach to approximate a cut locus would be to use a fast marching method which provides an efficient way to compute distance functions on a manifold. Unfortunately, classical algorithms do not ensure any convergence result related to the gradient of the approximation. We believe that this absence of estimate makes the approximation of the cut locus by these algorithms difficult to prove. In this article we introduce a new regularized approach designed to fill this gap and to obtain a reliable localization of the cut locus. Given a large constant $m > 0$, let $u_m \in H^1(S)$ be the minimizer of the following variational problem

$$\min_{\substack{u\in H^1(S)\\ |\nabla_S u|\le 1\\ u(b)=0}} \int_S \Big(|\nabla_S u|^2 - mu\Big), \tag{1.1}$$

where ∇_S denotes the gradient operator on the surface S. Intuitively, u_m is a mollification away from b of the distance function to the point b on S. For $\lambda > 0$ to be chosen small, we will use the set

$$E_{m,\lambda} := \left\{ x \in S \setminus \{b\} : |\nabla_S u_m(x)|^2 \le 1 - \frac{\lambda^2}{u_m^2(x)} \right\}$$

as an approximation of $\mathrm{Cut}_b(S)$. See Figure 1 for an illustration of the sensitivity of u_m and $E_{m,\lambda}$ with respect to parameters m and λ.

This is justified by some theoretical results obtained in [12], which will be summarized in Sections 3 and 4. The Sections 2–4 are devoted to explaining how we arrived at such a set $E_{m,\lambda}$. For now, let us give a bit of intuition about the different terms appearing in $E_{m,\lambda}$. When perturbing the surface S, we expect the same kind of instabilities as the ones observed in [3] in the case of the medial axis. Thus, two kinds of new points may appear in $\mathrm{Cut}_b(S)$:

(1) points where some minimizing geodesics meet with an angle close to zero,
(2) points that are near the base point b.

Hence, to make $\mathrm{Cut}_b(S)$ more stable (and so more computable), we need to select points that are not too close to b and such that some minimizing geodesics meet with an angle significantly larger than 0. Intuitively, having $|\nabla_S u_m(x)|^2 \le 1 - \alpha^2$ for some constant $\alpha > 0$ ensures that we are selecting points x where minimizing geodesics meet with an angle significantly larger than 0, and replacing α^2 by λ^2/u_m^2 ensures that we are selecting points that are away from b. Some other definitions of $E_{m,\lambda}$ would have been possible (for instance, the squares are not needed), and this form has been chosen as it corresponds to the λ-medial axis introduced in [7] (see Sect. 2).

The rest of the paper is organized as follows. In Section 2, we recall the notion of λ-medial axis that was introduced in [7] and summarize some of its properties. In Section 3, following the strategy of the λ-medial axis,

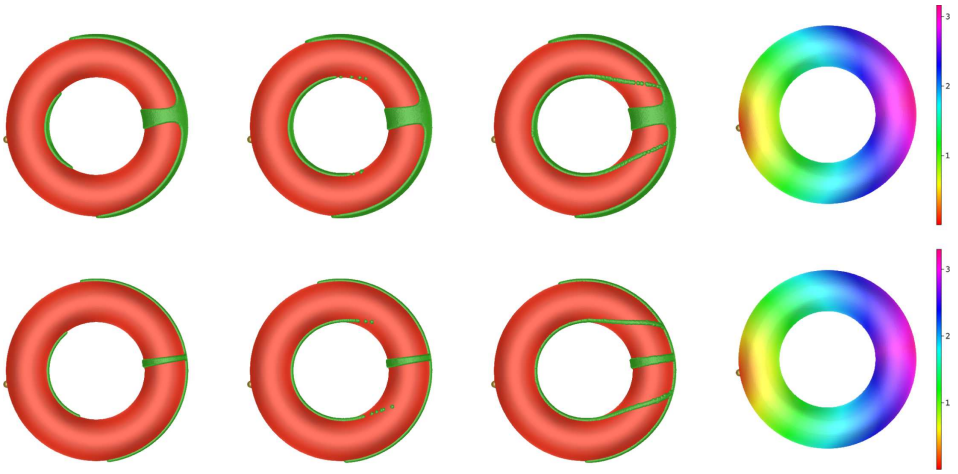

FIGURE 1. Approximation of the sets $E_{m,\lambda}$ (green color) for $m = 10$ (*first row*) and $m = 50$ (*second row*) for three different values of λ. The first three columns correspond to values of $\lambda = 0.6$, 0.2 and 0.06 respectively. The last column represents the associated solutions u_m.

we define a "λ-cut locus" $\mathrm{Cut}_b^\lambda(S)$ and show that it can be used as an approximation of the complete cut locus for λ small enough. In Section 4, we recall the result from [12] which states that the set $E_{m,\lambda}$ defined above is a good approximation of $\mathrm{Cut}_b^\lambda(S)$ if m is big enough. In Section 5, we discretize problem (1.1) using finite elements, to find a discrete minimizer $u_{m,h}$, where $h > 0$ is the step of the discretization. From this discrete minimizer $u_{m,h}$, we obtain a function $u_{m,h}^l$ on S, and we show that the set

$$E_{m,\lambda,h} := \left\{ x \in S \setminus \{b\} : \left|\nabla_s u_{m,h}^l(x)\right|^2 \leq 1 - \frac{\lambda^2}{\left(u_{m,h}^l\right)^2(x)} \right\},$$

is a good approximation of $E_{m,\lambda}$ as $h \to 0$. In Section 6, we present the results of some numerical experiments.

2. The λ-medial axis

In this section, we recall briefly the notion of λ-medial axis introduced by Chazal and Lieutier [7]. Given an open subset Ω of $\mathbb{R}^2$, its medial axis $\mathcal{M}(\Omega)$ is defined as the set of points of Ω that have at least two closest points on the boundary $\partial\Omega$ of Ω:

$$\mathcal{M}(\Omega) := \{x \in \Omega : \exists y, z \in \partial\Omega,\ y \neq z \text{ and } d_{\partial\Omega}(x) = |x - y| = |x - z|\},$$

where for any $x \in \Omega$, $d_{\partial\Omega}(x)$ is the distance from x to $\partial\Omega$:

$$d_{\partial\Omega}(x) = \min\left\{|x - y| \ :\ y \in \partial\Omega\right\}.$$

The medial axis $\mathcal{M}(\Omega)$ is unstable with respect to small non-smooth perturbations of the boundary of Ω. To deal with this issue, in [7] Chazal and Lieutier defined the so called λ-*medial axis* of Ω by setting, for any $\lambda > 0$,

$$\mathcal{M}_\lambda(\Omega) := \{x \in \Omega : r(x) \geq \lambda\}, \tag{2.1}$$

where $r(x)$ is the radius of the smallest ball containing the set of all closest points to x on $\partial\Omega$, *i.e.* the set $\{z \in \partial\Omega : |x - z| = d_{\partial\Omega}(x)\}$. The map $\lambda \mapsto \mathcal{M}_\lambda(\Omega)$ is nonincreasing, and

$$\mathcal{M}(\Omega) = \bigcup_{\lambda>0} \mathcal{M}_\lambda(\Omega).$$

It is further proved in Section 3, Theorem 2 of [7] that $\mathcal{M}_\lambda(\Omega)$ has the same homotopy type as $\mathcal{M}(\Omega)$, for λ small enough. These facts justify that $\mathcal{M}_\lambda(\Omega)$ is a good approximation of $\mathcal{M}(\Omega)$, for λ small enough. The crucial difference though is that $\mathcal{M}_\lambda(\Omega)$ is stable with respect to small variations of the boundary of Ω, whereas $\mathcal{M}(\Omega)$ is not. We refer the reader to Section 4 of [7] for precise statements and proofs.

To motivate the next section, we will also use an alternative definition of the λ-medial axis. Given a point $x \in \Omega$, let $\Theta(x)$ be the center of the smallest ball containing all the closest points to x on $\partial\Omega$. In Section 2.1 of [7], a vector field $\nabla d_{\partial\Omega}$ (originally denoted only by ∇) is defined on Ω by:

$$\nabla d_{\partial\Omega}(x) := \frac{x - \Theta(x)}{d_{\partial\Omega}(x)}.$$

This vector field coincides with the classical gradient of $d_{\partial\Omega}$ wherever $d_{\partial\Omega}$ is differentiable, so it can be thought of as a generalized gradient of $d_{\partial\Omega}$. Moreover, we have the following relation (see Eq. (1) in Sect. 2.1 of [7]):

$$|\nabla d_{\partial\Omega}(x)|^2 = 1 - \frac{r^2(x)}{d^2_{\partial\Omega}(x)}.$$

Therefore, we have the following equivalent definition of the λ-medial axis:

$$\mathcal{M}_\lambda(\Omega) = \left\{ x \in \Omega : |\nabla d_{\partial\Omega}(x)|^2 \leq 1 - \frac{\lambda^2}{d^2_{\partial\Omega}(x)} \right\}. \tag{2.2}$$

3. λ-Cut locus

We want to define a set similar to the λ-medial axis in the case of the cut locus $\mathrm{Cut}_b(S)$. To this end, we need a notion of generalized gradient for the distance function d_b. The notion of generalized gradient we use is presented in Section 1.3 of [16] in the context of Alexandrov spaces and in Section 2.2 of [12]. Here, we introduce the notion omitting the short proofs otherwise needed. First note that, as stated in Proposition 2.7 of [12], the function d_b is locally semiconcave on $S \setminus \{b\}$, which means that for any unit speed geodesic $\gamma : [0,1] \to S \setminus \{b\}$, there exists a constant $C > 0$ such that the function $t \mapsto Ct^2 - d_b(\gamma(t))$ is convex on $[0,1]$. From there, one gets that for any point $x \in S \setminus \{b\}$ and any direction $v \in T_xS$, d_b admits a directional derivative

$$\partial^+_v d_b(x) = \lim_{t \to 0^+} \frac{d_b(\exp_x(tv)) - d_b(x)}{t}$$

where $\exp_x$ denotes the Riemannian exponential map at x. Furthermore, for any $x \in S \setminus \{b\}$, the map $v \mapsto \partial^+_v d_b(x)$ admits a unique maximizer v_x on the closed ball $\overline{B}(0,1) \subset T_xS$. The generalized gradient of d_b is then defined as

$$\nabla_{_S} d_b(x) = \partial^+_{v_x} d_b(x) v_x.$$

What is more, we have the following formula

$$|\nabla_{_S} d_b(x)| = \max\left(0, \sup_{v \in T_xS, |v|=1} \partial^+_v d_b(x)\right). \tag{3.1}$$

See Lemma 3.3 for a geometric interpretation of the generalized gradient.

Analogously to (2.2), for $\lambda > 0$, we define the λ-cut locus as

$$\mathrm{Cut}_b^\lambda(S) := \left\{ x \in S \setminus \{b\} : |\nabla_S d_b(x)|^2 \leq 1 - \frac{\lambda^2}{d_b^2(x)} \right\}.$$

We have the following proposition from Proposition 2.9 of [12].

Proposition 3.1. *The map $\lambda \mapsto \mathrm{Cut}_b^\lambda(S)$ is nonincreasing, and*

$$\mathrm{Cut}_b(S) = \overline{\bigcup_{\lambda>0} \mathrm{Cut}_b^\lambda(S)}.$$

In addition, the following proposition holds. We recall that $\mathrm{Cut}_b(S)$ is always connected (see [15] for instance).

Proposition 3.2. *If S is a real analytic surface, then for $\lambda > 0$ small enough, one of the connected components of $\mathrm{Cut}_b^\lambda(S)$ has the same homotopy type as $\mathrm{Cut}_b(S)$, while the other connected components, if any, are contractible.*

These two propositions justify that $\mathrm{Cut}_b^\lambda(S)$ is a good approximation of $\mathrm{Cut}_b(S)$, for $\lambda > 0$ small enough. Before proving Proposition 3.2, we prove the following lemma.

Lemma 3.3. *Let $x \in \mathrm{Cut}_b(S)$ be such that there exist two unit speed minimizing geodesics $\gamma_1, \gamma_2 : [0, d_b(x)] \to S$ such that $\gamma_i(0) = b$ and $\gamma_i(d_b(x)) = x$. Let $\theta \in (0, \pi]$ be the angle between γ_1 and γ_2 at x. Then, we have*

$$|\nabla_S d_b(x)| \leq \cos(\theta/2).$$

Proof. For $i = 1, 2$, let us set $v_i = -\dot{\gamma}_i(d_b(x))$. Let us denote by $\exp_x$ the Riemannian exponential map at the point x. Let $t_0 \in (0, d_b(x))$ and $x_i = \exp_x(v_i t_0)$. Note that we have $x \notin \mathrm{Cut}_{x_i}(S)$, so the function d_{x_i} is smooth at x, and its gradient is $-v_i$. Given $v \in T_x S$ such that $|v| = 1$, using $d_b(x) = d_{x_i}(x) + d_b(x_i)$, we have

$$\begin{aligned}
\partial_v^+ d_b(x) &= \lim_{t \to 0^+} \frac{d_b(\exp_x(vt)) - d_b(x)}{t} \\
&\leq \lim_{t \to 0^+} \frac{d_{x_i}(\exp_x(vt)) + d_b(x_i) - (d_{x_i}(x) + d_b(x_i))}{t} \\
&= \lim_{t \to 0^+} \frac{d_{x_i}(\exp_x(vt)) - d_{x_i}(x)}{t} \\
&= -v \cdot v_i.
\end{aligned}$$

Given that the angle between v_1 and v_2 is θ, there exists $i \in \{1, 2\}$, such that the angle between v and v_i is at most $\pi - \theta/2$. Thus the last inequality gives $\partial_v^+ d_b(x) \leq \cos(\theta/2)$. This concludes the proof. □

Remark 3.4. In the previous lemma, in the case where there are exactly two minimizing geodesics arriving at x, one can show that the inequality is an equality.

Using Lemma 3.3, Proposition 3.2 will mainly be a consequence of Proposition 3.4 from [9], which is recalled in Proposition 3.6 below. Following [9], we will use the following terminology. Let G be a finite connected graph embedded in S. A point x of a finite connected graph G is called a *tree point* if x is a leaf of G or $G \setminus \{x\}$ has a connected component whose closure is a tree. Otherwise, x is called a *cycle point*. As shown in the proof of Proposition 3.5 from [9], the closure of the set of cycle points of a finite connected graph G is a deformation retract of G, hence it is connected. We will also use the following lemma.

Lemma 3.5. *Let G be a finite connected graph. Let $\mathcal{C} \subset G$ be a closed connected set that contains all cycle points of G. Then $\mathcal{C}$ is a deformation retract of G.*

Proof. Let $T_1, \dots, T_k$ be the connected components of $G \setminus \mathcal{C}$. As $\mathcal{C}$ contains all cycle points of G, for any $1 \leq i \leq k$, T_i is a tree and $\overline{T_i} \cap \mathcal{C}$ is a singleton $\{x_i\}$. By contracting all T_i to their roots x_i, we obtain that $\mathcal{C}$ is a deformation retract of G. □

Let $x \in S$ be such that there exist two minimizing unit speed geodesics γ_1 and γ_2 from b to x. Following [9], the *spread* between γ_1 and γ_2 is defined as

$$spd(\gamma_1, \gamma_2) = \sup_t d(\gamma_1(t), \gamma_2(t)).$$

We recall that, as S is real analytic, the cut locus $\mathrm{Cut}_b(S)$ is a finite graph (see [15] in dimension 2 and [5] for the generalization to arbitrary dimensions). In [9], the authors proved the following:

Proposition 3.6 ([9], Prop. 3.4)**.** *Let $x \in \mathrm{Cut}_b(S)$. If the spread of any two minimizing unit speed geodesics γ_1 and γ_2 from b to x is smaller than the injectivity radius of S, then x is a tree point of $\mathrm{Cut}_b(S)$.*

Proof of Proposition 3.2. According to Lemma 3.3, given any $\theta > 0$, if λ has been taken small enough, then for any point $x \in \mathrm{Cut}_b(S) \setminus \mathrm{Cut}_b^\lambda(S)$, the angle between any two minimizing unit speed geodesics γ_1 and γ_2 from b to x is smaller than θ at x. As geodesics verify a second order differential equation, if their angle at x is small, then their spread is also small. Therefore, applying Proposition 3.6, we deduce that if λ has been taken small enough, then any point $x \in \mathrm{Cut}_b(S) \setminus \mathrm{Cut}_b^\lambda(S)$ is a tree point of $\mathrm{Cut}_b(S)$. Stated otherwise, $\mathrm{Cut}_b^\lambda(S)$ contains all cycle points of $\mathrm{Cut}_b(S)$. Moreover, $\mathrm{Cut}_b^\lambda(S)$ is a closed set. Indeed, this is a consequence of the semiconcavity of d_b and the lower semicontinuity of the norm of the gradient of semiconcave functions (see [12], Prop. 7.2). Thus, $\mathrm{Cut}_b^\lambda(S)$ contains the closure of the cycle points of $\mathrm{Cut}_b(S)$, which is connected. In particular, there exists a connected component $\mathcal{C}$ of $\mathrm{Cut}_b^\lambda(S)$ that contains the set of the cycle points of $\mathrm{Cut}_b(S)$. By Lemma 3.5, $\mathcal{C}$ is a deformation retract of $\mathrm{Cut}_b(S)$. This completes the proof. □

Therefore, we will use $\mathrm{Cut}_b^\lambda(S)$ as an approximation of $\mathrm{Cut}_b(S)$ for λ small enough.

4. Approximation with a variational problem

For $m > 0$, recall that u_m is the minimizer in (1.1). For $\lambda > 0$, let us define the set $E_{m,\lambda}$ by

$$E_{m,\lambda} := \left\{ x \in S \setminus \{b\} : |\nabla_S u_m(x)|^2 \leq 1 - \frac{\lambda^2}{u_m^2(x)} \right\}.$$

We have the following theorem (see [12], Thms. 1.1 and 1.3):

Theorem 4.1. *There exists $m_0 > 0$ such that for any $m > m_0$, the function u_m is locally $C^{1,1}$ on $S \setminus \{b\}$, and $u_m = d_b$ in a neighborhood of b. For any $m > m' > m_0$,*

$$\mathrm{Cut}_b(S) \subset \{|\nabla_S u_m| < 1\} \subset \{|\nabla_S u_{m'}| < 1\}. \tag{4.1}$$

Moreover,

$$\{|\nabla_S u_m| < 1\} \underset{m \to +\infty}{\longrightarrow} \mathrm{Cut}_b(S) \quad \text{in the Hausdorff sense.} \tag{4.2}$$

Finally, for any $\varepsilon > 0$,

$$\sup_{x \in E_{m,\lambda}} d\Big(x, \mathrm{Cut}_b^\lambda(S)\Big) \underset{m \to +\infty}{\longrightarrow} 0, \quad \text{and} \quad \sup_{x \in \mathrm{Cut}_b^{\lambda+\varepsilon}(S)} d(x, E_{m,\lambda}) \underset{m \to +\infty}{\longrightarrow} 0. \tag{4.3}$$

Therefore, we can use $E_{m,\lambda}$ as an approximation of $\mathrm{Cut}_b^\lambda(S)$. All in all, we will use $E_{m,\lambda}$ as an approximation of $\mathrm{Cut}_b(S)$.

In the following, we will always assume that we have $m > m_0$.

5. Discretization

5.1. Finite elements of order r on a surface approximation of order k

In this section we introduce a discretization framework adapted to the variational problem (1.1), based on finite elements. We follow the notations of [8,11].

Let S be a compact oriented smooth two-dimensional surface embedded in $\mathbb{R}^3$. For $x \in S$, we denote by $\nu(x)$ the oriented normal vector field on S. Let $d : \mathbb{R}^3 \to \mathbb{R}$ be the signed distance function to the surface S and $U_\eta = \{x \in \mathbb{R}^3, |d(x)| < \eta\}$ the tubular neighborhood of S of width $\eta > 0$. It is well known that if η is small enough (for instance $0 < \eta < \min_{i=1,2} \frac{1}{|\kappa_i|_{L^\infty(S)}}$ where the (κ_i) stand for the extremal principal curvatures of S), then for every $x \in U_\eta$, there exists a unique $a(x) \in S$ such that

$$x = a(x) + d(x)\nu(a(x)) = a(x) + d(x)\nabla d(x). \tag{5.1}$$

We consider S_h a triangular approximation of S whose vertices lie on S and whose faces are quasi-uniform and shape regular of diameter at most $h > 0$. Moreover, we will assume that $\mathcal{T}_h$, the set of triangular faces of S_h, are contained in some tubular neighborhood U_η such that the map a defined by (5.1) is unique.

For $k \geq 1$ and for a triangle $T \in \mathcal{T}_h$, we consider the n_k Lagrange basis functions $\Phi_1^k, \dots \Phi_{n_k}^k$ of degree k and define the discrete projection on S_h by:

$$a_k(x) = \sum_{j=1}^{n_k} a(x_j)\Phi_j^k(x) \tag{5.2}$$

where $x_1, \dots, x_{n_k}$ are the nodal points associated to the basis functions. Now we can define S_h^k a polynomial approximation of order k of S associated to $\mathcal{T}_h$

$$S_h^k = \{a_k(x),\, x \in S_h\}. \tag{5.3}$$

Observe that by definition the image by a of the nodal points are both on S and on S_h^k. Let us now introduce the finite element spaces on $S_h = S_h^1$ and S_h^k for $k \geq 2$. For every integer $r \geq 1$, let

$$L_h^r = \left\{\chi \in C^0(S_h),\, \chi|_T \in \mathbb{P}_r, \forall T \in \mathcal{T}_h\right\} \tag{5.4}$$

where $\mathbb{P}_r$ is the family of polynomials of degree at most r. Analogously, for $k \geq 2$, let

$$L_h^{r,k} = \left\{\hat{\chi} \in C^0(S_h^k),\, \hat{\chi} = \chi \circ a_k^{-1}, \text{ for some } \chi \in L_h^r\right\}. \tag{5.5}$$

Analogously to (1.1), we will consider the following discrete variational problem:

$$\min_{\substack{u \in L_h^{r,k} \\ \left|\nabla_{S_h^k} u\right| \leq 1 \\ u(b)=0}} F_h^k(u) \tag{5.6}$$

where $F_h^k(u) = \int_{S_h^k} \left(\left|\nabla_{S_h^k} u\right|^2 - mu \right)$ and b some fixed nodal point of the mesh $\mathcal{T}_h$.

5.2. Convergence of the lifted minimizers

In order to prove the convergence of our numerical approach, let us first establish that our discrete problem converges in values in the sense of Proposition 5.2. For a function u defined on S_h^k, we introduce its lifted function u^l defined on S, by the relation $u^l(a(x)) = u(x)$.

We focus our analysis on the piecewise linear case $r = k = 1$. We will use the notation $F_h := F_h^1$ and $L_h := L_h^1$. For every $h > 0$, the convex optimization problem (5.6) has a unique solution $u_{m,h}$.

Lemma 5.1. *The differential of the projection $a : U_\eta \to \mathbb{R}^3$ onto S, when restricted to the tangent space of S_h, is the identity, up to order 1 in h:*

$$Da_{|_{TS_h}} = Id^{|\mathbb{R}^3}_{|_{TS_h}} + \mathcal{O}(h).$$

Proof. The identity estimate on Da is a direct consequence of [11] equations (4.12), (4.13), (4.10) and (4.11). □

Defining $F(u) = \int_S \Big(|\nabla_S u|^2 - mu \Big)$, we have the following proposition.

Proposition 5.2. *Let $u_{m,h}$ be the solution of problem (5.6) for $k = r = 1$. Let $Lu^l_{m,h} := \frac{u^l_{m,h}}{\max\left(|\nabla_S u^l_{m,h}|_{L^\infty(S)},1\right)}$ be the 1-Lipschitz normalization of $u^l_{m,h}$. Then, $Lu^l_{m,h} \in H^1(S)$ and*

$$F\big(Lu^l_{m,h}\big) = \min_{\substack{u\in H^1(S)\\ |\nabla_S u|\le 1\\ u(b)=0}} F(u) + \mathcal{O}\Big(h^{\frac{1}{2}}\Big).$$

Proof. **Step 1.** Let u_m be the solution of problem (1.1). For $\varepsilon > 0$, let $w_{m,\varepsilon} : S \to \mathbb{R}$ be defined by:

$$w_{m,\varepsilon} = \begin{cases} \frac{d_b(x)^2}{2\varepsilon} & \text{if} \quad d_b(x) \le \varepsilon \\ u_m(x) - \frac{\varepsilon}{2} & \text{if} \quad d_b(x) \ge \varepsilon. \end{cases}$$

Recall that we have $u_m = d_b$ in a neighborhood of b (Thm. 4.1). Therefore, for $\varepsilon > 0$ small enough, we have $u_m = d_b$ on the ball $B(b, 2\varepsilon)$. In particular, we deduce that $w_{m,\varepsilon}$ is C^1 on S. As d_b^2 is smooth in a neighborhood of b, the gradient of $d_b^2/2\varepsilon$ is $\mathcal{O}(\varepsilon^{-1})$-Lipschitz on $B(b, \varepsilon)$. Moreover, as $u_m = d_b$ on $B(b, 2\varepsilon)$, the gradient of u_m is $\mathcal{O}(\varepsilon^{-1})$-Lipschitz on $B(b, 2\varepsilon) \setminus B(b, \varepsilon)$. Recall that u_m is also locally $C^{1,1}$ on $S \setminus \{b\}$ (Thm. 4.1). Therefore its gradient is $\mathcal{O}(\varepsilon^{-1})$-Lipschitz on $S \setminus B(b, \varepsilon)$. All in all, we obtain that $w_{m,\varepsilon}$ is $C^{1,1}$ on S and the Lipschitz constant of its gradient is $\mathcal{O}(\varepsilon^{-1})$. Furthermore, as d_b and u_m are both 1-Lipschitz, we have $|\nabla_S w_{m,\varepsilon}| \le 1$. Now for $\varepsilon > 0$, consider

$$v_{h,\varepsilon} := \frac{I_h w_{m,\varepsilon}}{\Big|\nabla_{S_h} I_h w_{m,\varepsilon}\Big|_{L^\infty(S_h)}},$$

where $I_h w_{m,\varepsilon}$ is the $\mathbb{P}^1$ Lagrange interpolation of $w_{m,\varepsilon}$ on S_h. Therefore, $v_{h,\varepsilon}$ is an admissible candidate in the minimization problem (5.6). For $x \in S_h$, observe that we have the relation $I_h w_{m,\varepsilon}(x) = I_h(w_{m,\varepsilon} \circ a)(x)$ which says that $I_h w_{m,\varepsilon}$ is the standard (flat) interpolation of the composed function $w_{m,\varepsilon} \circ a$. As the map $a : U_\eta \to S$ is smooth and the gradient of $w_{m,\varepsilon}$ is $\mathcal{O}(\varepsilon^{-1})$-Lipschitz, we deduce that on every triangle of S_h, the gradient of $w_{m,\varepsilon} \circ a$ is $\mathcal{O}(\varepsilon^{-1})$-Lipschitz, uniformly in h. By the quasi uniformity of the mesh, we obtain the uniform interpolation estimates on S_h:

$$I_h w_{m,\varepsilon}(x) = (w_{m,\varepsilon} \circ a)(x) + \mathcal{O}\big(\varepsilon^{-1} h^2\big) \tag{5.7}$$

and

$$\nabla_{S_h} I_h w_{m,\varepsilon}(x) = \nabla_{S_h}(w_{m,\varepsilon} \circ a)(x) + \mathcal{O}\big(\varepsilon^{-1} h\big).$$

With Lemma 5.1, we deduce for all $x \in S_h$,

$$\nabla_{S_h} I_h w_{m,\varepsilon}(x) = \nabla_S w_{m,\varepsilon}(a(x)) + \mathcal{O}\big(\varepsilon^{-1} h\big). \tag{5.8}$$

Recall that we have $|\nabla_S w_{m,\varepsilon}|_{L^\infty(S)} = 1$. Therefore the last identity yields

$$\left|\nabla_{S_h} I_h w_{m,\varepsilon}\right|_{L^\infty(S_{h,\varepsilon})} = 1 + \mathcal{O}\big(\varepsilon^{-1}h\big).$$

Thus, $v_{h,\varepsilon} = I_h w_{m,\varepsilon}\big(1 + \mathcal{O}\big(\varepsilon^{-1}h\big)\big)$, and so

$$F_h(v_{h,\varepsilon}) = F_h(I_h w_{m,\varepsilon}) + \mathcal{O}\big(\varepsilon^{-1}h\big). \tag{5.9}$$

Applying Lemma 5.1 again, with a simple change of variable, we find that for any function $f : S \to \mathbb{R}$,

$$\int_{S_h} f \circ a = \int_S f + \mathcal{O}(h). \tag{5.10}$$

Recalling (5.7) and (5.8), we obtain

$$F_h(I_h w_{m,\varepsilon}) = F(w_{m,\varepsilon}) + \mathcal{O}\big(\varepsilon^{-1}h\big). \tag{5.11}$$

Furthermore, we have

$$\int_S |w_{m,\varepsilon} - u_m| \le \mathcal{O}(\varepsilon) \quad \text{and} \int_S \Big||\nabla_S w_{m,\varepsilon}|^2 - |\nabla_S u_m|^2\Big| \le \mathcal{O}(\varepsilon^2),$$

so

$$F(w_{m,\varepsilon}) = F(u_m) + \mathcal{O}(\varepsilon).$$

Combining this with (5.9) and (5.11), we find

$$F_h(v_{h,\varepsilon}) = F(u_m) + \mathcal{O}\big(\varepsilon^{-1}h\big) + \mathcal{O}(\varepsilon).$$

Choosing $\varepsilon = h^{\frac{1}{2}}$, this yields

$$\min_{\substack{u\in L_h \\ \left|\nabla_{S_h} u\right|\le 1 \\ u(b)=0}} F_h(u) \le \min_{\substack{u\in H^1(S) \\ |\nabla_S u|\le 1 \\ u(b)=0}} F(w) + \mathcal{O}\Big(h^{\frac{1}{2}}\Big). \tag{5.12}$$

Step 2. Let $u_{m,h}$ be the solution of the discrete problem (5.6), $u^l_{m,h} := u_{m,h} \circ (a_{|S_h})^{-1}$ its lifted version on S, and

$$Lu^l_{m,h} := \frac{u^l_{m,h}}{\max\Big(\Big|\nabla_S u^l_{m,h}\Big|_{L^\infty(S)}, 1\Big)}.$$

Using the equation $u_{m,h} = u^l_{m,h} \circ a$ and Lemma 5.1 as before, we obtain that uniformly for $x \in S_h$,

$$\nabla_S u^l_{m,h} \circ a(x) = \nabla_{S_h} u_{m,h}(x) + \mathcal{O}(h). \tag{5.13}$$

In particular, this implies

$$\big|\nabla_S u^l_{m,h}\big|_{L^\infty(S)} = \Big|\nabla_{S_h} u_{m,h}\Big|_{L^\infty(S_h)} + \mathcal{O}(h) \le 1 + \mathcal{O}(h),$$

and so

$$Lu^l_{m,h} = u^l_{m,h}(1 + \mathcal{O}(h)). \tag{5.14}$$

From this identity we deduce

$$F\big(Lu^l_{m,h}\big) = F\big(u^l_{m,h}\big) + \mathcal{O}(h).$$

Using the estimates (5.13) and (5.10) as in step one, we find

$$F_h(u_{m,h}) = F\big(u^l_{m,h}\big) + \mathcal{O}(h).$$

The last two equations together yield $F\Big(Lu^l_{m,h}\Big) = F_h(u_{m,h}) + \mathcal{O}(h)$. With (5.12), this implies

$$\min_{\substack{u\in H^1(S)\\ |\nabla_S u|\le 1\\ u(b)=0}} F(u) \le F\big(Lu^l_{m,h}\big) \le \min_{\substack{u\in H^1(S)\\ |\nabla_S u|\le 1\\ u(b)=0}} F(u) + \mathcal{O}\Big(h^{\frac{1}{2}}\Big),$$

which concludes the proof of the proposition.

□

In the proof of the next proposition, we will need the following lemma.

Lemma 5.3. *Let $L > 0$. Let $(f_h)_{h>0}$ be a family of L-Lipschitz real functions on S such that $|\nabla f_h|_{L^1(S)} \to 0$ as $h \to 0$ and for any $h > 0$, $f_h(b) = 0$. Then*

$$|f_h|_{L^1(S)} \underset{h\to 0}{\longrightarrow} 0.$$

Proof. Let $\varepsilon > 0$ and $S_\varepsilon := S \setminus (\mathrm{Cut}_b(S) \cup B(b,\varepsilon))$. We will use the polar coordinates (r,θ) centered at b on S_ε. In these coordinates, the surface measure on S_ε is of the form $\mathrm{d}\mathcal{A} = A(r,\theta)\mathrm{d}r\mathrm{d}\theta$, with

$$A(r,\theta) \underset{r\to 0}{\sim} r, \quad \text{uniformly in } \theta. \tag{5.15}$$

Moreover, the surface S_ε is of the form

$$S_\varepsilon = \{(r,\theta), \theta \in [0,2\pi), r \in [\varepsilon, r_\theta)\},$$

for some $r_\theta > 0$ that depends on $\theta \in [0,2\pi)$. As the $(f_h)_{h>0}$ are L-Lipschitz and $f_h(b) = 0$, we have for any $\theta \in [0,2\pi)$, $|f_h(\varepsilon,\theta)| \le L\varepsilon$. Using this inequality, we have

$$\begin{aligned}
\int_{S_\varepsilon} |f_h| &= \int_0^{2\pi}\int_\varepsilon^{r_\theta} |f_h(r,\theta)| A(r,\theta)\mathrm{d}r\mathrm{d}\theta \\
&\le \int_0^{2\pi}\int_\varepsilon^{r_\theta} |f_h(r,\theta) - f_h(\varepsilon,\theta)| A(r,\theta)\mathrm{d}r\mathrm{d}\theta + \int_0^{2\pi}\int_\varepsilon^{r_\theta} |f_h(\varepsilon,\theta)| A(r,\theta)\mathrm{d}r\mathrm{d}\theta \\
&\le \int_0^{2\pi}\int_\varepsilon^{r_\theta} |f_h(r,\theta) - f_h(\varepsilon,\theta)| A(r,\theta)\mathrm{d}r\mathrm{d}\theta + \mathcal{A}(S)L\varepsilon \\
&= \int_0^{2\pi}\int_\varepsilon^{r_\theta} \left|\int_\varepsilon^{r} \partial_r f_h(t,\theta)\mathrm{d}t\right| A(r,\theta)\mathrm{d}r\mathrm{d}\theta + \mathcal{A}(S)L\varepsilon \\
&\le \int_0^{2\pi}\int_\varepsilon^{r_\theta}\int_\varepsilon^{r} |\nabla f_h(t,\theta)|\mathrm{d}t A(r,\theta)\mathrm{d}r\mathrm{d}\theta + \mathcal{A}(S)L\varepsilon.
\end{aligned} \tag{5.16}$$

From (5.15), we know that for some constants $C_1, C_2 > 0$, we have for any $r > 0$ and $\theta \in [0,2\pi)$, $C_1 r \le A(r,\theta) \le C_2$. In particular, for $r \ge t \ge \varepsilon$, we get

$$A(r,\theta) \le C_2 \le C_2\frac{t}{\varepsilon} \le \frac{C_2}{C_1\varepsilon}A(t,\theta).$$

Setting $C := C_2/C_1$, with (5.16), we find

$$\begin{aligned}\int_{S_\varepsilon} |f_h| &\leq \frac{C}{\varepsilon}\int_0^{2\pi}\int_\varepsilon^{r_\theta}\int_\varepsilon^{r} |\nabla f_h(t,\theta)|A(t,\theta)\mathrm{d}t\mathrm{d}r\mathrm{d}\theta + \mathcal{A}(S)L\varepsilon \\ &= \frac{C}{\varepsilon}\int_0^{2\pi}\int_\varepsilon^{r_\theta}\int_t^{r_\theta} |\nabla f_h(t,\theta)|A(t,\theta)\mathrm{d}r\mathrm{d}t\mathrm{d}\theta + \mathcal{A}(S)L\varepsilon \\ &\leq \frac{C\,\mathrm{diam}(S)}{\varepsilon}\int_0^{2\pi}\int_\varepsilon^{r_\theta} |\nabla f_h(t,\theta)|A(t,\theta)\mathrm{d}t\mathrm{d}\theta + \mathcal{A}(S)L\varepsilon \\ &= \frac{C\,\mathrm{diam}(S)}{\varepsilon}\int_{S_\varepsilon} |\nabla f_h| + \mathcal{A}(S)L\varepsilon, \end{aligned} \tag{5.17}$$

where $\mathrm{diam}(S)$ is the diameter of S. Note that because the $(f_h)_{h>0}$ are L-Lipschitz and $f_h(b) = 0$, we have

$$\int_S |f_h| = \int_{S_\varepsilon} |f_h| + \int_{B(b,\varepsilon)} |f_h| \leq \int_{S_\varepsilon} |f_h| + \mathcal{A}(S)L\varepsilon.$$

Therefore the estimate (5.17) yields

$$\int_S |f_h| \leq \frac{C\,\mathrm{diam}(S)}{\varepsilon}\int_S |\nabla f_h| + 2\mathcal{A}(S)L\varepsilon.$$

In particular, for any $\varepsilon > 0$,

$$\limsup_{h\to 0}\int_S |f_h| \leq 2\mathcal{A}(S)L\varepsilon.$$

This concludes the proof. □

We can now establish the convergence of the minimizers:

Proposition 5.4.

$$\left|\nabla_S u^l_{m,h} - \nabla_S u_m\right|^2_{L^2(S)} = \mathcal{O}\left(h^{\frac{1}{2}}\right) \quad \text{and} \quad \left|u^l_{m,h} - u_m\right|_{L^1(S)} \underset{h\to 0}{\longrightarrow} 0.$$

Proof. Consider $v = \frac{1}{2}\left(Lu^l_{m,h} + u_m\right)$. Then, v is admissible for problem (1.1), so $F(v) \geq F(u_m)$. Moreover, the following algebraic identity holds

$$F(v) = \frac{1}{2}F\left(Lu^l_{m,h}\right) + \frac{1}{2}F(u_m) - \frac{1}{4}\int_S \left|\nabla_S u_m - \nabla_S Lu^l_{m,h}\right|^2.$$

Therefore, we have

$$\frac{1}{2}F\left(Lu^l_{m,h}\right) - \frac{1}{2}F(u_m) \geq \frac{1}{4}\int_S \left|\nabla_S u_m - \nabla_S Lu^l_{m,h}\right|^2,$$

which proves, together with Proposition 5.2, that

$$\left|\nabla_S Lu^l_{m,h} - \nabla_S u_m\right|^2_{L^2(S)} = \mathcal{O}\left(h^{\frac{1}{2}}\right). \tag{5.18}$$

In particular, as S is compact, the gradient of the function $Lu^l_{m,h} - u_m$ also goes to 0 in the $L^1(S)$ norm as $h \to 0$. Recall that the functions $\left(Lu^l_{m,h}\right)_{h>0}$ and u_m are uniformly Lipschitz, and $Lu^l_{m,h}(b) = u_m(b) = 0$, so we may apply Lemma 5.3 to the functions $(Lu^l_{m,h} - u_m)_{h>0}$, to find that

$$\left|Lu^l_{m,h} - u_m\right|_{L^1(S)} \underset{h\to 0}{\longrightarrow} 0. \tag{5.19}$$

In the proof of Proposition 5.2, we showed that $Lu^l_{m,h} = u^l_{m,h}(1 + \mathcal{O}(h))$ (Eq. (5.14)). Together with (5.18) and (5.19), this concludes the proof. □

We just proved that the gradient of the lifted minimizers of the discrete problems (5.6) converge with an order at least 1/4 to the gradient of the minimizer of problem (1.1).

5.3. Convergence in measure of $E_{m,\lambda,h}$

Let us recall that the set $E_{m,\lambda}$ is defined by

$$E_{m,\lambda} = \left\{ x \in S \setminus \{b\} : |\nabla_S u_m(x)|^2 \leq 1 - \frac{\lambda^2}{u_m^2(x)} \right\}.$$

Proposition 5.5. *For any $\lambda > 0$, let us define*

$$E_{m,\lambda,h} := \left\{ x \in S \setminus \{b\} : \left|\nabla_S u^l_{m,h}(x)\right|^2 \leq 1 - \frac{\lambda^2}{\left(u^l_{m,h}\right)^2(x)} \right\}.$$

For any $\varepsilon > 0$ with $\varepsilon < \lambda/2$, we have

$$|E_{m,\lambda+\varepsilon} \setminus E_{m,\lambda,h}| = \mathcal{O}\left(h^{\frac{1}{4}}\right) \quad \text{and} \quad |E_{m,\lambda,h} \setminus E_{m,\lambda-\varepsilon}| = \mathcal{O}\left(h^{\frac{1}{4}}\right).$$

Proof. By definition of $E_{m,\lambda}$ and $E_{m,\lambda,h}$, we have

$$E_{m,\lambda+\varepsilon} \setminus E_{m,\lambda,h} \subset \left\{ \left|\nabla_S u^l_{m,h}\right|^2 - |\nabla_S u_m|^2 > \frac{(\lambda+\varepsilon)^2}{u_m^2} - \frac{\lambda^2}{\left(u^l_{m,h}\right)^2} \right\}.$$

Therefore, on $E_{m,\lambda+\varepsilon} \setminus E_{m,\lambda,h}$, we have

$$\begin{aligned} \left|\nabla_S u^l_{m,h}\right|^2 - |\nabla_S u_m|^2 &> \frac{(\lambda+\varepsilon)^2 - \lambda^2}{u_m^2} + \lambda^2 \left(\frac{1}{u_m^2} - \frac{1}{\left(u^l_{m,h}\right)^2} \right) \\ &\geq \frac{2\varepsilon\lambda + \varepsilon^2}{(\mathrm{diam}(S))^2} + \lambda^2 \left(\frac{1}{u_m^2} - \frac{1}{\left(u^l_{m,h}\right)^2} \right), \end{aligned} \tag{5.20}$$

where $\mathrm{diam}(S)$ is the diameter of S. Recall that, by Proposition 5.4, $u^l_{m,h}$ converges to u_m in $L^1(S)$ as h goes to 0. As the functions u_m and $u^l_{m,h}$ are uniformly Lipschitz, this implies that $u^l_{m,h}$ converges to u_m in $L^\infty(S)$. Moreover, by definition of $E_{m,\lambda}$, we also have $E_{m,\lambda+\varepsilon} \subset \{u_m \geq (\lambda+\varepsilon)\}$, so on $E_{m,\lambda+\varepsilon} \setminus E_{m,\lambda,h}$, the difference $\left(\frac{1}{u_m^2} - \frac{1}{\left(u^l_{m,h}\right)^2} \right)$ converges uniformly to 0 as h goes to 0. With (5.20), this implies that for h small enough, we have on $E_{m,\lambda+\varepsilon} \setminus E_{m,\lambda,h}$,

$$\left|\nabla_S u^l_{m,h}\right|^2 - |\nabla_S u_m|^2 \geq \frac{2\varepsilon\lambda + \varepsilon^2}{2(\mathrm{diam}(S))^2}.$$

In particular, setting $\eta := \frac{2\varepsilon\lambda+\varepsilon^2}{2(\mathrm{diam}(S))^2}$ and using Proposition 5.4, we obtain

$$\begin{aligned} |E_{m,\lambda+\varepsilon} \setminus E_{m,\lambda,h}| &\leq \left| \left\{ \left|\nabla_S u^l_{m,h}\right|^2 - |\nabla_S u_m|^2 > \eta \right\} \right| \\ &\leq \frac{1}{\eta} \int_S \left| \left|\nabla_S u^l_{m,h}\right|^2 - |\nabla_S u_m|^2 \right| \\ &= \mathcal{O}\left(h^{\frac{1}{4}}\right). \end{aligned}$$

This concludes the proof of the first estimate. The other estimate is proved by the same method. □

FIGURE 2. Artifacts using low order approximation.

Remark 5.6. The function u_m is generically suspected to be no more than $\mathcal{C}^{1,1}$ regular. This important difficulty makes the extension of the previous convergence analysis to higher order elements not straightforward. However, based on our numerical experiments (see the following paragraph), we believe that a (k, r) approximation improves the order of convergence without being able to provide a complete analysis of this order due to this lack of regularity.

Sections 3–5 together justify the claim that the set $E_{m,\lambda,h}$ is a good approximation of the cut locus of b in S, if m is big enough and λ and h are small enough. We tried to estimate numerically the order of convergence of our approximation. Unfortunately, the precision of our simulations was not enough to determine if the expected order of convergence $1/4$ is optimal or not.

6. Numerical illustrations

6.1. Cut locus approximation

We established the convergence of the minimizers of problem (5.6) when h tends to 0. For a fixed $h > 0$, this convex discrete problem is of quadratic type with an infinite number of conic pointwise constraints. By the way, it is important to observe that for $k = r = 1$, the gradient pointwise bounds for a function of $\mathbb{P}^1$ is equivalent to a single discrete conic constraint on every triangle with respect to the degrees of freedom of $\mathbb{P}^1(\mathcal{T}_h)$. In this simplified context, we observed in our experiments that using $\mathbb{P}^1$ elements may lead to approximated cut loci with some tiny artificial connected components (see Fig. 2). Observe that these artifacts do not contradict our convergence estimates in Proposition 5.5. Motivated by this lack of precision, we use in all following illustrations elements of order $r > 1$.

For the general case $r > 1$, the bound constraint on the gradient cannot be easily reduced to a finite set of discrete constraints. In our computations, we approximated the constraint $|\nabla_{S_h^k} u|_{L^\infty(S_h^k)} \leq 1$ by forcing the inequality only on a finite number of points of the mesh. In practice, we imposed these constraints on g Gauss quadrature points on every triangle of $\mathcal{T}_h$.

We illustrate in Figures 3–6 the approximation of the cut locus provided by our approach. These computations have been carried out on meshes of approximately 10^5 triangles for $k = 2$ and $r = 3$ using a high precision quadrature formula associated to 17 Gauss points on every element of the mesh. Moreover, for $r = 3$, we imposed the conic gradient constraints on the $g = 9$ Gauss points of every triangle. In order to solve the resulting linear conic constrained quadratic optimization problem, we used the *JuMP* modeling language and the finite elements library *Getfem++* [10, 17] combined with the *MOSEK* optimization solver [2]. For such a precision, the optimization solver identified a solution in less than one hour on a standard computer.

Observe that our approximations of cut loci provide sets with a number of handles equal to twice the genus of the supporting surfaces. This fact is in agreement with Proposition 3.2 since the cut locus has he same homotopy group as the surface (see [6] for instance).

FIGURE 3. Three different views of the approximation of a cut locus on a standard torus.

FIGURE 4. Three different views of the approximation of a cut locus on a standard torus, without representing the surface.

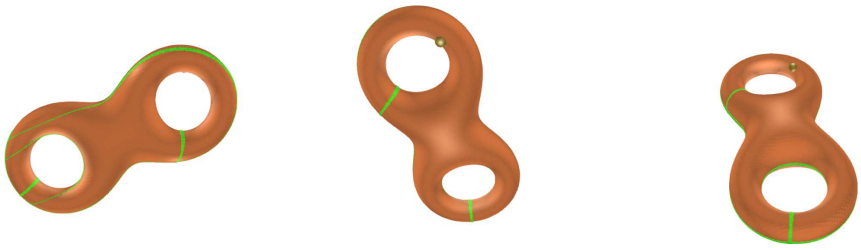

FIGURE 5. Three different views of the approximation of a cut locus on a torus of genus 2.

FIGURE 6. Three different views of the approximation of a cut locus on a torus of genus 2, without representing the surface.

6.2. Approximation of the boundary of Voronoi cells

All previous theoretical results still hold if we replace the source point b by any compact subset of the surface S. For instance, if b is replaced by a set of points, the singular set of the distance function can be decomposed as the union of the boundary of Voronoi cells and the cut loci of every point intersected with its Voronoi cell. As a consequence, if the distribution of source points is homogeneous enough, that is every Voronoi cell is small enough, the singular part of the distance function will be exactly equal to the boundary of the Voronoi cells. We illustrate this remark in the following experiments. We used exactly the same framework as in previous sections and just replaced the pointwise condition at b with the analogous pointwise Dirichlet conditions at every source

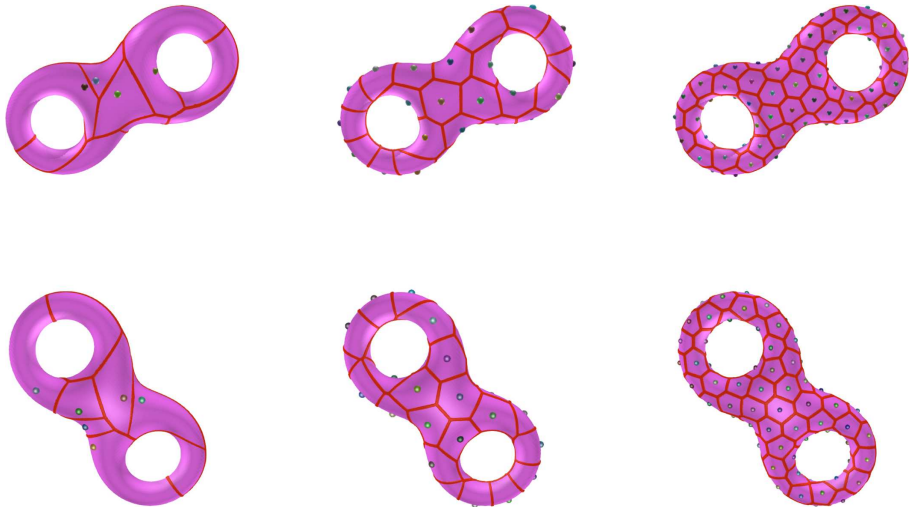

FIGURE 7. Approximation of the Voronoi cells on a torus of genus 2 of 10, 30 and 100 points. Every column represents two different views.

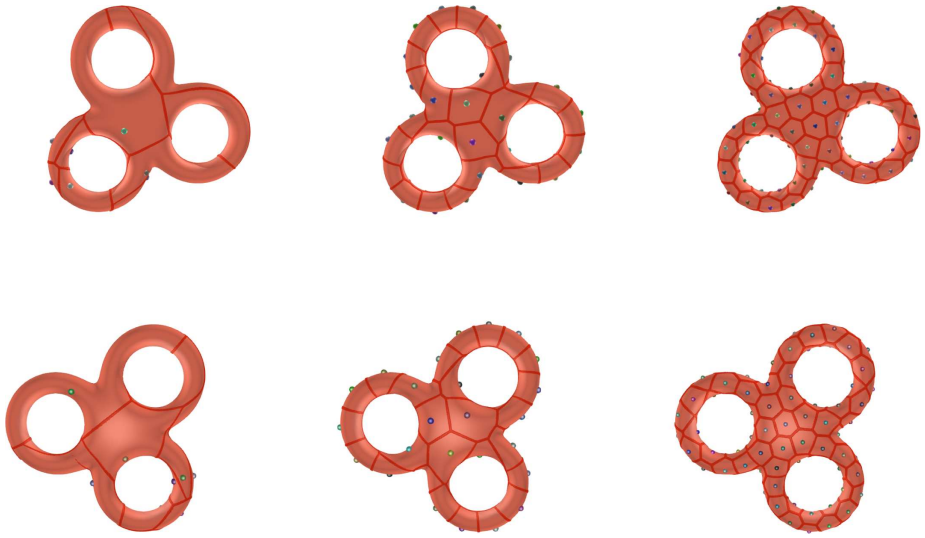

FIGURE 8. Approximation of the Voronoi cells on a torus of genus 3 of 10, 30 and 100 points. Every column represents two different views.

point. Figures 7 and 8 represent the Voronoi diagrams obtained with 10, 30 and 100 points for surfaces of genus 2 and 3. The computational complexity is exactly of the same order as with a single source point.

Acknowledgements. The three authors were partially supported by Agence Nationale de la Recherche (ANR) with the projects GeoSpec (LabEx PERSYVAL-Lab, ANR-11-LABX-0025-01), CoMeDiC (ANR-15-CE40-0006) and ShapO (ANR-18-CE40-0013). The third author is supported by the European Research Council (ERC), under the European Union's Horizon 2020 research and innovation programme, through the project ERC VAREG – *Variational approach to the regularity of the free boundaries* (grant agreement No. 853404).

References

[1] P. Albano, On the stability of the cut locus. *Nonlinear Anal. Theory Methods App.* **136** (2016) 51–61.

[2] E.D. Andersen and K.D. Andersen, The mosek interior point optimizer for linear programming: an implementation of the homogeneous algorithm. In: High Performance Optimization. Springer (2000) 197–232.

[3] D. Attali and A. Montanvert, Modeling noise for a better simplification of skeletons. In: Proceedings of 3rd IEEE International Conference on Image Processing. Vol. 3. IEEE (1996) 13–16.

[4] B. Bonnard, O. Cots and L. Jassionnesse, Geometric and numerical techniques to compute conjugate and cut loci on Riemannian surfaces. In: Geometric Control Theory and Sub-Riemannian Geometry. Springer (2014) 53–72.

[5] M.A. Buchner, Simplicial structure of the real analytic cut locus. *Proc. Am. Math. Soc.* **64** (1977) 118–121.

[6] I. Chavel, Riemannian Geometry: A Modern Introduction. Vol. 98. Cambridge University Press (2006).

[7] F. Chazal and A. Lieutier, The "λ-medial axis". *Graphical Models* **67** (2005) 304–331.

[8] A. Demlow, Higher-order finite element methods and pointwise error estimates for elliptic problems on surfaces. *SIAM J. Numer. Anal.* **47** (2009) 805–827.

[9] T.K. Dey and K. Li, Cut locus and topology from surface point data. In: Proceedings of the Twenty-Fifth Annual Symposium on Computational Geometry. ACM (2009) 125–134.

[10] I. Dunning, J. Huchette and M. Lubin, Jump: a modeling language for mathematical optimization. *SIAM Rev.* **59** (2017) 295–320.

[11] G. Dziuk and C.M. Elliott, Finite element methods for surface PDEs. *Acta Numer.* **22** (2013) 289–396.

[12] F. Générau, E. Oudet and B. Velichkov, Cut locus on compact manifolds and uniform semiconcavity estimates for a variational inequality. Preprint arXiv:2006.07222 [math] (2020).

[13] J.-I. Itoh and R. Sinclair, Thaw: a tool for approximating cut loci on a triangulation of a surface. *Exp. Math.* **13** (2004) 309–325.

[14] M.K. Misztal, J.A. Bærentzen, F. Anton and S. Markvorsen, Cut locus construction using deformable simplicial complexes. In: 2011 Eighth International Symposium on Voronoi Diagrams in Science and Engineering. IEEE (2011) 134–141.

[15] S.B. Myers, Connections between differential geometry and topology II. Closed surfaces. *Duke Math. J.* **2** (1936) 95–102.

[16] A. Petrunin, Semiconcave functions in Alexandrov's geometry. *Surv. Differ. Geom.* **11** (2006) 137–202.

[17] Y. Renard and J. Pommier, Getfem++. An open source generic C++ library for finite element methods (http://home.gna.org/getfem) (2006).

[18] R. Sinclair and M. Tanaka, Loki: software for computing cut loci. *Exp. Math.* **11** (2002) 1–25.